Journal of Applied Polymer Science

Co-electrospun nanofibers of PVA-SbQ and Zein for wound healing

Jing Cui,[1] Liying Qiu,[2] Yuyu Qiu,[1,2] Qingqing Wang,[1] Qufu Wei[1]
[1]Key Laboratory of Eco-textiles, Jiangnan University, China
[2]Laboratory of Natural Medicine, School of Pharmaceutical Science, Jiangnan University, China
Correspondence to: Q. Wei; (E-mail: qfwei@jiangnan.edu.cn)

ABSTRACT: In this study, electrospun biocompatible nanofibers with random orientation were prepared by physically blending poly(-vinyl alcohol)-stilbazol quaternized (PVA-SbQ) with zein in acetic acid solution for wound healing. PVA-SbQ was used as the foundation polymer as well as crosslinking agent, blended with zein to achieve desirable properties such as improved tensile strength, surface wettability, and *in vitro* degradable properties. Moreover, vaccarin drug was incorporated in situ into electrospun nanofibrous membranes for cell viability and cell attachment. The addition of vaccarin showed great effects on the morphology of nanofiber and enhanced cell viability and proliferation in comparison with composite nanofibers without drug. The presence of PVA-SbQ, zein, and vaccarin drug in the nanofibrous membranes exhibited good compatibility, hydrophilicity, and biocompatibility and created a moist environment to have potential application for wound healing. © 2015 Wiley Periodicals, Inc. J. Appl. Polym. Sci. **2015**, *132*, 42565.

KEYWORDS: biocompatibility; electrospinning; fibers

Received 1 March 2015; accepted 31 May 2015
DOI: 10.1002/app.42565

INTRODUCTION

Recently, nanofibers have attracted a great deal of attention and shown huge potential as dressings for wound care.[1–3] The ideal wound dressing materials could accelerate the healing process, prevent infection, and restore the structure and function of the skin.[4] Because of the nanometer-size distribution and random alignment of the fibers, nanofibers would be able to mimic the structure of the natural extracellular matrix (ECM),[5] which could encourage the proliferation of epithelial cells and the formation of new tissue.[6] Moreover, the properties of specific surface area ratio and high porosity with tunable pore size facilitate fluid absorption, cell respiration, and high-gas permeation.[7,8] Generally, nanofibers can be fabricated by various methods and perhaps electrospinning is the most facile route because of its one-step process.[9] By utilizing electrostatic field between spinneret and collector provided by a high voltage supply, fibers with sizes ranging from nanometers to a few microns can be fabricated. Through the electrically charged fluid jet, solvent gets evaporated and the resultant fibers are collected. In addition, due to the ease of implementation, simplicity, cost-effectiveness, flexibility, potential to scale up, and ability to spin a broad range of polymers, electrospinning technique has versatile potential applications for tissue engineering,[10] wound dressing,[11] drug delivery,[12,13] guided bone regeneration,[14] enzyme immobilization.[15] Among the various potential applications, wound dressing is one of the most promising uses. Up to now, various polymers and biopolymers have been electrospun into nanofibers and widely used in the field of wound dressing.[16,17] Unnithan *et al.* studied the electrospun PU-CA-zein composite mats for wound dressing whereas PU was used as the foundation polymer.[18] Naseri *et al.* investigated the electrospun chitosan-based nanocomposite mats reinforced with chitin nanocrystals for dressing materials.[6] Lin *et al.* developed biocompatible co-electrospun nanofibrous membranes of collagen and zein for wound healing.[3]

Zein, a predominantly corn-based protein, exhibits various properties such as biocompatible, biodegradable, resistance to microbial attack, high thermal resistance, great oxygen barrier properties as well as excellent film-forming capabilities.[19] It is generally regarded as safe "GRAS" status.[20] Such properties make zein be investigated for a number of applications such as drug delivery,[21] packaging sector,[22] and tissue engineering.[23] However, the poor mechanical properties of zein have drastically restricted its further applications, especially those involving mechanical tolerances. Studies showed that using plasticizers (e.g., triethylene glycol) or crosslinking reagents (e.g., glyoxal, glutaraldehyde) could improve the mechanical property of zein.[24–26] However, these crosslinking agents are not as green as needed, while their products suffer from significantly diminished elongation properties. Other relatively green crosslinking reagents have been reported, such as hexamethylenediisocyanate (HDI),[27] polycarboxylic acids,[28] carbodiimide,[29] to name a few. Yet, the final products still suffer from either a lack of either one or a combination of mechanical properties

or environmental friendliness. In our previous study, we developed a novel atom efficient and green two-step crosslinking process using the crosslinking properties of SbQ, which is a green amphiphilic sensitizer of the styrylpyridinium family, can be dimerized via an atom economic [2+2] orbitally conserved cycloaddition reaction triggered by UV radiation.[30] SbQ is typically reported along with poly(vinyl alcohol) (PVA) as a covalently grafted pendant group on a polymer backbone forming poly(vinyl alcohol)-stilbazol quaternized (PVA-SbQ).[31] There are several reports about using PVA-SbQ for drug delivery.[32,33] Liu *et al.* first investigated the electrospinning of PVA-SbQ with PVA for potential application of drug delivery.[34]

In this study, PVA-SbQ was used as the foundation polymer and crosslinking agent, blended with zein to obtain desirable properties such as enhanced mechanical properties, better biocompatibility and cell adhesion, improved hydrophilicity. Vaccarin, a major flavonoid glycoside in Vaccariae semen, can attenuate endothelial cell oxidative stress injury in association with neovascularization in vitro and in vivo.[35] It was incorporated into the electrospun nanofibers for the first time. The study demonstrated the process, stability, compatibility, and the characterization of the composite nanofibers with drug and without drug. The electrospun nanofibrous membranes containing vaccarin can be used as wound healing materials.

EXPERIMENTAL

Materials

Poly(vinyl alcohol)-stilbazol quaternized (PVA-SbQ) ($M_w = 45{,}000$) was supplied from Shanghai Guangyi Printing Equipment Technology (China). Zein ($M_w = 35{,}000$) was purchased from Sigma-Aldrich (St. Louis, MO) Company. Acetic acid was received from Sinopharm Chemical Reagent (China). Vaccarin was purchase from Shanghai Shifeng technology (Shanghai, China). The mouse fibroblast (L929) cells were obtained from the cell bank of Chinese Academy of Sciences. Deionized water was used for the preparation of all solutions.

Methods

For the electrospinning, pure zein and PVA-SbQ solution were prepared in aqueous 70% (v/v) acetic acid and deionized water, respectively. A different ratio of zein powder commingled with PVA-SbQ was weighed and dissolved in aqueous 70% (v/v) acetic acid solution at room temperature. After being vigorously stirred for 1 h upon, a homogeneous solution was obtained. The total polymer concentration of each solution for the electrospinning was maintained at 40% (v/v). The solutions were placed in a pump syringe with a stainless steel needle. The applied voltage was 25 kV with a working distance of 15 cm from the needle tip to the surface of the aluminum foil used as a collector site (circular rotating drum), and the flow rate of the solution was 1 mL/h. The electrospun membranes were irradiated under a POWER ARC UV100 Lamp for specific time to get the crosslinked ones. The compositional characteristics of the as-spun nanofibrous membranes were demarcated as zein (control), PVA-SbQ/zein (1 : 1), PVA-SbQ/zein (2 : 1), PVA-SbQ/zein (3 : 1), PVA-SbQ/zein (4 : 1). For the in situ incorporation of vaccarin drug, a required amount of vaccarin was dissolved in the PVA-SbQ/zein (1 : 1) blend and then coelectrospun at the same condition to PVA-SbQ/zein/drug composite membranes. To ensure the acetic acid did not remain in the electrospun fibers, the fibers were dried in a vacuum dryer for 24 h at room temperature to remove the solvent.

Characterizations

Morphological and Physical Analysis. Scanning electron microscopy (SEM, Quanta 200, Holland FEI Company) was used to investigate the surface morphology of the zein, PVA-SbQ/zein, and PVA-SbQ/zein/drug composite membranes. The samples were sputter coated with a thin layer of gold before the SEM imaging. Diameters of the electrospun nanofibers were measured by Adobe Acrobat 7.0 professional from SEM images, while 100 fibers were analyzed for each sample to obtain an average fiber diameter.

The shear viscosity of the electrospinning solutions was measured by using a rotating viscometer (Physica MCR301, ANTON PAAR GMBH). The temperature of the solutions was kept at 25°C by a water jacket and a thermostatically controlled water bath. The measurements were made at multiple spindle rotational speeds to determine the rheological behavior of the solutions. Every reading was recorded after 10 spindle rotations to reach equilibrium. For each applied rotational speed, viscosity (cP), shear rate (s^{-1}), and torque (%) values were recorded.

The thermal properties of the nanofibers were investigated by differential scanning calorimetry (DSC) (TA-Q2000) and thermal gravimetric analysis (TGA) (TA-Q5000). DSC analyses were carried out with approximately 6 mg of samples under N_2 as a purge gas. Initially, the samples were equilibrated at 25°C then they were heated to 200°C at a heating rate of 10°C/min. TGA was performed from room temperature to 700°C at a heating rate of 10°C/min under nitrogen.

Mechanical Properties. Mechanical properties of the zein, PVA-SbQ/zein composite membranes were tested using a uniaxial testing machine (INSTRON1185) at a crosshead speed of 10 mm/min and gauge length of 5 cm. The samples were cut in rectangular form and the tested samples were about 10 cm in length, 1 cm in width. The thicknesses of the samples were measured using a DUALSCOPE MPO digital micrometer having a precision of 1 μm. The results were an average based on at least five tests for each material.

Chemical Analysis. The chemical functional groups in the range of 4000–750 cm^{-1} of nanofibers were investigated by Fourier transform infrared spectroscopy (FTIR, Nicolet Nexus, Thermo Electron Corporation) using ATR reflection. The spectra were recorded with 16 scans at a resolution of 4 cm^{-1}.

Degradation and Surface Wettability Measurement. The in vitro degradation of electrospun PVA-SbQ/zein membranes were measured by immersing the fibers in a phosphate buffer (pH = 7.4) at 37°C. The samples were removed from the solutions and weighed at 7, 14, 21 days after dried inside an oven for 24 h. The weight lost (WL, %) of the nanofibrous membranes was calculated according to the following eq. (1):

$$\mathrm{WL}\ (\%) = (W_0 - W_1)/W_0 \times 100 \quad (1)$$

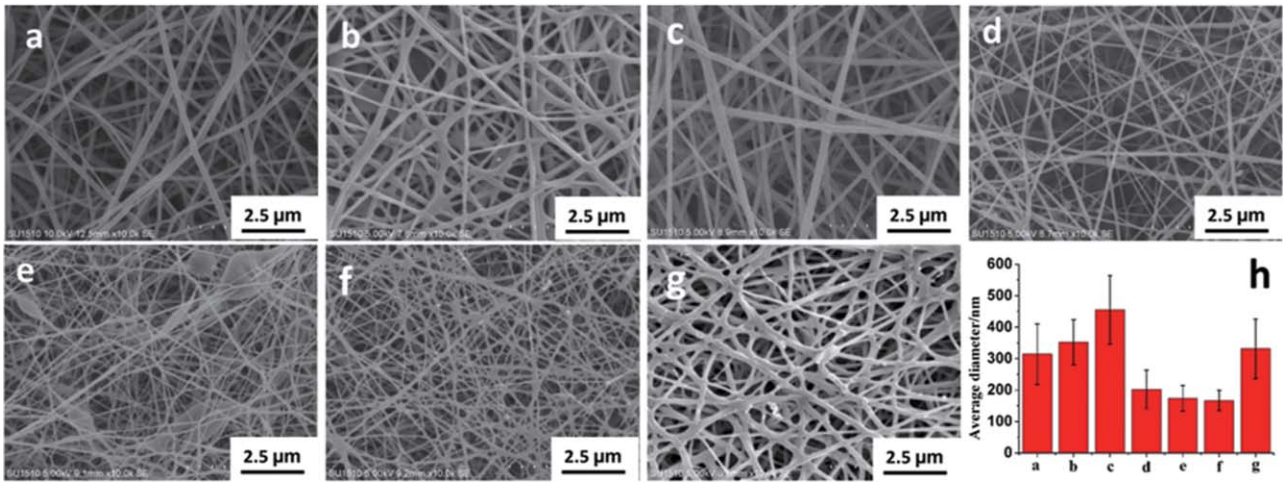

Figure 1. SEM images of electrospun (a) zein (control), (b) PVA-SbQ, (c) PVA-SbQ/zein (1 : 1), (d) PVA-SbQ/zein (2 : 1), (e) PVA-SbQ/zein (3 : 1), (f) PVA-SbQ/zein (4 : 1), (g) PVA-SbQ/zein (1 : 1)/drug nanofibers, (h) nanofibers diameter distribution. [Color figure can be viewed in the online issue, which is available at wileyonlinelibrary.com.]

where W_0 and W_1 are initial weight of the fiber sample and the weight of fiber sample in different days, respectively.

The water contact angle of each fiber sample was measured to characterize the surface wettability using a surface tension meter (DCAT21, Delta Phase, Germany).

In Vitro Cytotoxicity Evaluation

Cell Viability Study. The L929 (mouse fibroblast) cells were used for the cell viability experiments. Cells were initially maintained in Dulbecco's Modified Eagle's Medium (DMEM), supplemented with 10% (w/v) fetal bovine serum, 100 μg/mL penicillin, and 100 μg/mL streptomycin. The dishes were incubated at 37°C in a humidified atmosphere of 5% CO_2 and the culture medium was changed once every 3 days.

Changes in cell viability produced by nanofibers were evaluated by indirect and direct cytotoxicity tests of the MTT assay. The indirect method was carried out by seeding L929 cells in to 96-well plates followed by incubation overnight. Electrospun mats were cut into the films with the area of ~1 cm^2 and sterilized by ethanol evaporation for 24 h. Different doses of DMEM were used to incubate the sterilized membranes according to ISO10993. After incubation, 100 μL of the media extract was transferred into each well. For direct cytotoxicity tests, 1.5 diameter membranes were incubated with 1 mL culture medium in 24-well plates for 24 h and L929 cells were seeded onto the nanofibers at a density of 4.0×10^5 cells/well.

Cells from the indirect tests were incubated for 24 h and 72 h and tested with MTT assay. The randomly chosen fields of cells were photographed at 100× amplification under a microscope video system (Olympus, IX70, Japan). The optical densities were measured at 570 nm with a 630 nm reference wavelength using a microplate spectrophotometer(EPOCH, Bio Tek Instruments, Highland Park). At each time point, six samples were used to measure the number of the viable cells. The percentage of viable cells was calculated using the following formula (2):

$$\%\ \text{cell viability} = A_{\text{nanofibers}}/A_{\text{control}} \times 100 \qquad (2)$$

where $A_{\text{nanofibers}}$ is the absorbance at 570 nm of the cells with nanofibers, and A_{control} is the absorbance at 570 nm of the control cells.

Cell Attachment Studies. The growth of L929 cells on the nanofibers was qualitatively analyzed using SEM described above. To observe cell attachment manner on the nanofibers, chemical fixation of cells was carried out in each sample. After 3 days of incubation, the nanofiber scaffolds were rinsed twice with PBS and subsequently fixed in 2.5% glutaraldehyde for 1 h. After that the samples were rinsed with deionized water and then dehydrated with ethanol. Finally, the samples were kept in a vacuum oven and then sputter coated with gold for the cell morphology observation by using SEM.

RESULTS AND DISCUSSION

Morphological and Physical Analysis

The surface morphology of the nanofibrous membranes is shown in Figure 1. Figure 1(a) represents the SEM image of pure zein nanofibers and Figure 1(b) is the image of pure PVA-SbQ. Figure 1(c–f) showed the SEM images of electrospun PVA-SbQ/zein with different ratios of 1 : 1, 2 : 1, 3 : 1, and 4 : 1, respectively. The SEM image of PVA-SbQ/zein with a ratio of 1:1 after adding vaccarin drug was shown in Figure 1(g). From Figure 1(h), we can get that the average diameter of all the nanofibers. The pure zein nanofibers demonstrated a smooth structure and had a wide diameter distribute with an average diameter of 314 ± 96 nm while pure PVA-SbQ nanofibers had an average diameter of 352 ± 72 nm. It also can be seen that the average diameter of co-electrospun PVA-SbQ /zein (1 : 1) nanofibers was higher than pure zein and PVA-SbQ nanofibers. With the decrease of zein from 50% to 20%, the average fiber diameter decreased from 455 nm to 167 nm, and the fibers became more adhesive. Furthermore, PVA-SbQ/zein (1 : 1) could be electrospun effectively into bead-free membranes with fibrous morphology and different fiber diameters. However, with the increase of PVA-SbQ amount and the decrease of zein amount, there were some beads morphology on

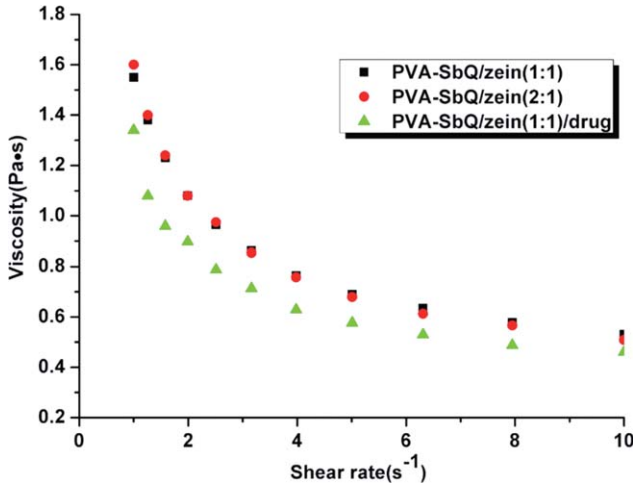

Figure 2. Viscosity of the electrospinning solutions as a function of shear rate in logarithmic scale. [Color figure can be viewed in the online issue, which is available at wileyonlinelibrary.com.]

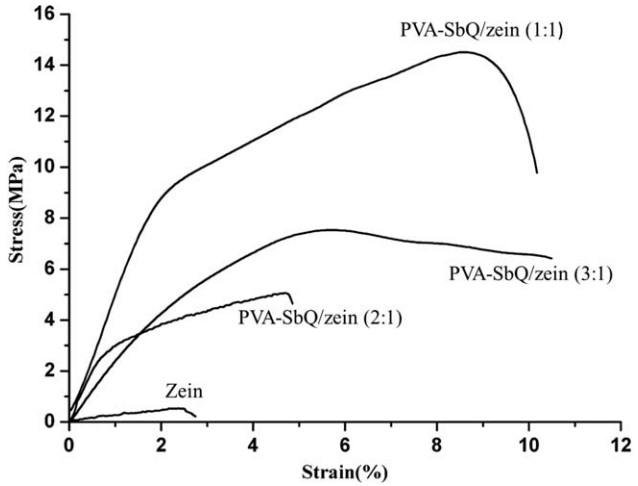

Figure 4. Stress–strain curves of pure zein nanofibers and PVA-SbQ/zein composite nanofibers.

the surface of the nanofibers. This was because the decrease of zein concentration lowered the electrospinnability.[19] It can be also observed that the addition of drug affected the morphology of the randomly oriented as-spun nanofibers and the porosity looked higher.

The morphology of the nanofibrous membranes was associated with the rheological properties of the electrospinning solutions which were investigated and the results of steady-shear flow are shown in Figure 2. It shows that while the shear rate increased, the viscosity of both electrospinning solutions decreased, suggesting a pseudoplastic non-Newtonian behavior, as it is usually observed for most polymer solutions.[36] Before the shear rate of 3 s^{-1}, the viscosity of the PVA-SbQ/zein (1 : 1) solution was a little lower than that of PVA-SbQ/zein (2 : 1) solution. After the addition of vaccarin drug, the viscosity of the solution decreased significantly during the shear rate range.

TGA tests were performed to determine the thermal properties of the components and composite nanofibers, which is shown in Figure 3. Decomposition of zein occurred between 275 and 350°C, which was in the range of the results reported in the literature of zein.[22] PVA-SbQ showed a three step degradation process. The first minor weight loss step up to 130°C was due to the removal of moisture and water molecules.[19] The second weight loss step (280∼360°C) was associated with the degradation of ester units of PVA. The third weight loss step (400–470°C) was ascribed to the dissociation of both inter and intra molecular forces with slight PVA-SbQ backbone degradation. For the PVA-SbQ/zein nanofibers, it showed more thermal stability, only existing a decomposition range between 300 and 400°C. The stability of drug cladding in the nanofibers could be improved.

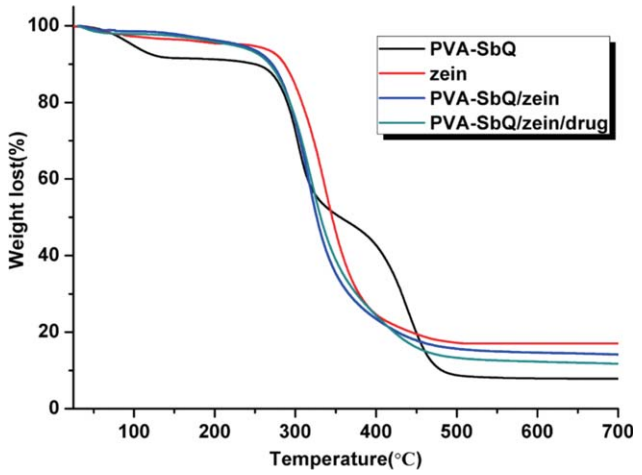

Figure 3. TGA graphs of pure PVA-SbQ, zein nanofibers, PVA-SbQ/zein, and PVA-SbQ/zein/drug nanofibers. [Color figure can be viewed in the online issue, which is available at wileyonlinelibrary.com.]

Mechanical Analysis

Figure 4 shows the stress strain curves of pristine zein and composite electrospun membranes. From the viewpoint of wound dressing application, electrospinning PVA-SbQ/zein membranes should have reasonable tensile strength and elongation at break.[37] A higher tensile strength and a greater elongation at break are considered to be important for practical handling and replacement during the wound healing process.[3] Pure zein presented poor elasticity and strength compared to PVA-SbQ/zein composite nanofibers. For the different ratio of PVA-SbQ and zein, PVA-SbQ/zein (1 : 1) exhibited the best mechanical properties. As observed from the SEM images in Figure 1, randomly oriented nanofibers of PVA-SbQ/zein (1 : 1) showed the smooth and bead-free morphology which could contribute to the mechanical properties.

Chemical Analysis

Compatibility among the components is essential for producing high-quality and stable of drug-loaded fibers. Second-order interactions, such as electrostatic interactions, hydrogen bonding and hydrophobic interactions would often improve this compatibility, which was investigated by Fourier transform infrared spectroscopy analysis (Figure 5). PVA-SbQ, zein, and vaccarin molecules possess free hydroxyl (acting as potential proton donors for hydrogen bonding) and carbonyl (potential proton receptors) groups [Figure 5(b)].[38] Therefore, hydrogen-bonding

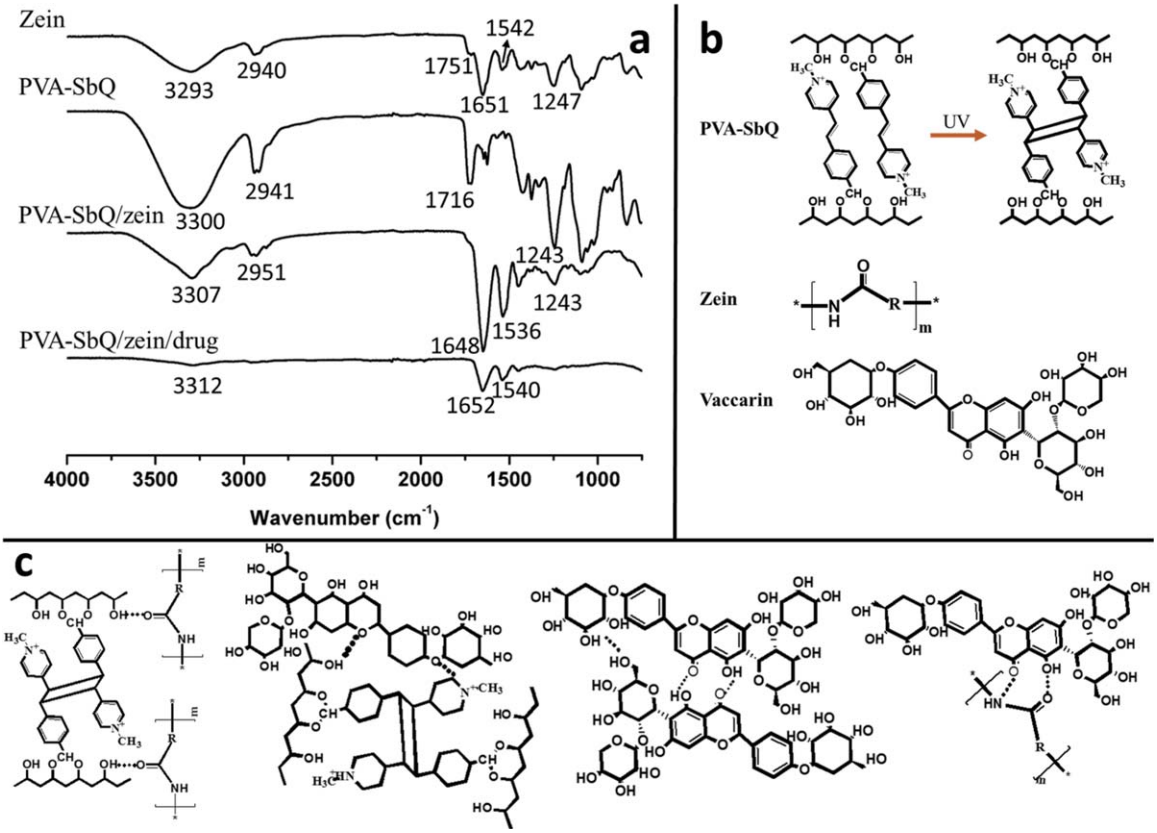

Figure 5. Compatibility investigation: (a) ATR-FTIR spectra of the components (zein, PVA-SbQ) and their composite nanofibers; (b) molecular structures of PVA-SbQ, zein, vaccarin; (c) hydrogen bonding between PVA-SbQ-zein, vaccarin-PV-SbQ, vaccarin-vaccarin, and vaccarin-zein. [Color figure can be viewed in the online issue, which is available at wileyonlinelibrary.com.]

interactions may occur within the composite nanofibers [Figure 5(c)]. From the ATR-FTIR spectra [Figure 5(a)], it shows that zein exhibited characteristic peaks at 3293 cm^{-1}, 1651 cm^{-1} (amide 1), 1542 cm^{-1} (amide 2), 1247 cm^{-1} (amide 3),which corresponded to the N–H stretching vibrations, C=O stretching, C–N stretching and N–H in plane deformation, respectively.[19] The spectrum of drug displayed characteristic peaks at 3450 cm^{-1}, 1654 cm^{-1} corresponding to the O–H stretching vibrations and Acyl bond. As for the PVA-SbQ/zein nanofibers, the absorption appears of the C=C groups at 1243 cm^{-1} was weakened, which confirmed that the photocrosslinking reaction of PVA-SbQ after UV radiation.[32,33] The

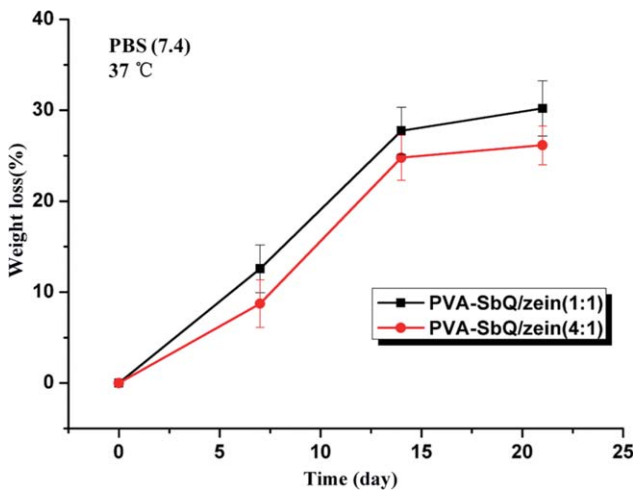

Figure 6. In vitro degradation profiles of electrospun nanofibers in a phosphate buffer solution (pH 7.4) at 37°C. [Color figure can be viewed in the online issue, which is available at wileyonlinelibrary.com.]

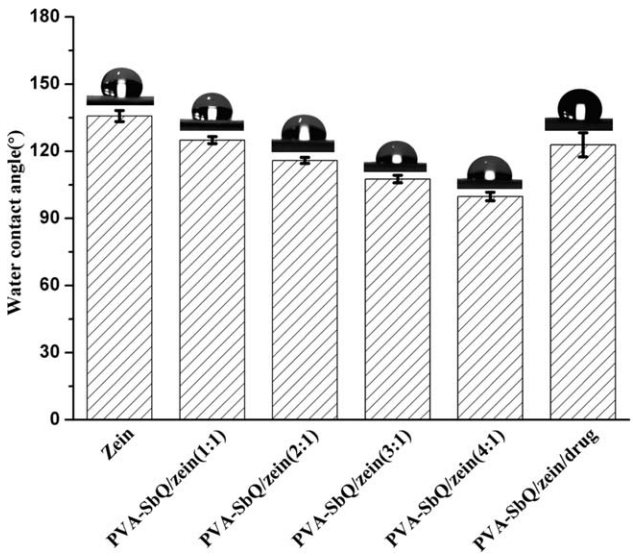

Figure 7. Water contact angles of electrospun nanofibers.

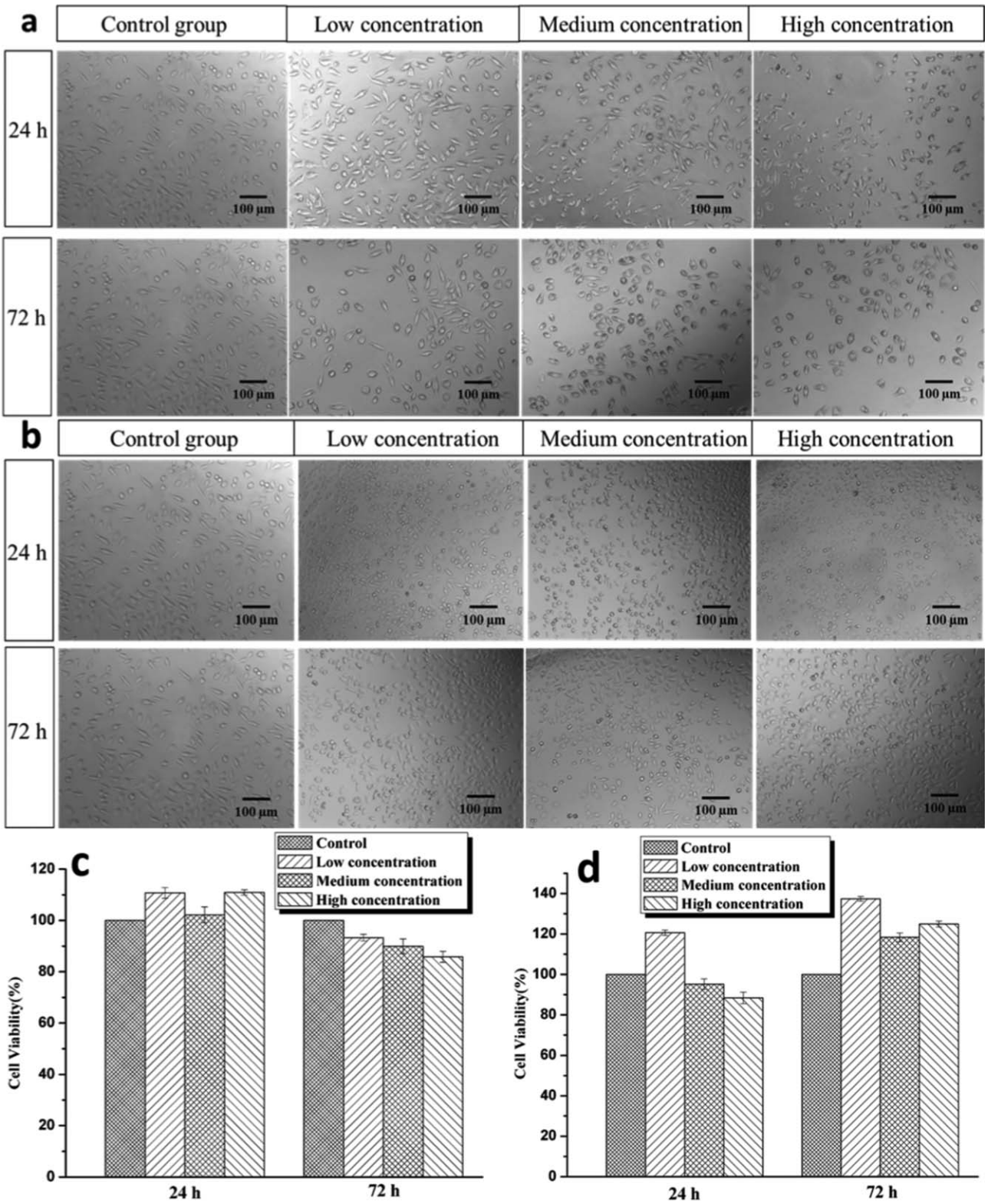

Figure 8. Cytotoxicity of nanofibers towards L929 cells with the indirect method: Microphotographs of PVA-SbQ/zein nanofibers (a) and PVA-SbQ/zein/drug nanofibers (b); MTT cell growth measurement assay. Cell viability of PVA-SbQ/zein nanofibers (c) and PVA-SbQ/zein/drug nanofibers (d). The viability of control cells was set at 100%. Values are mean ± SD.

cycloadditon reaction of the double bonds in SbQ initiated by UV radiation was expected to produce a three-dimensional (3D) structure which promoted the molecular entanglement. In the ATR-FTIR spectrum of PVA-SbQ/zein/drug nanofibers, the amide 2 band tended to shift to lower frequency at about 1532 cm^{-1}. These results indicated that stable-sheet secondary

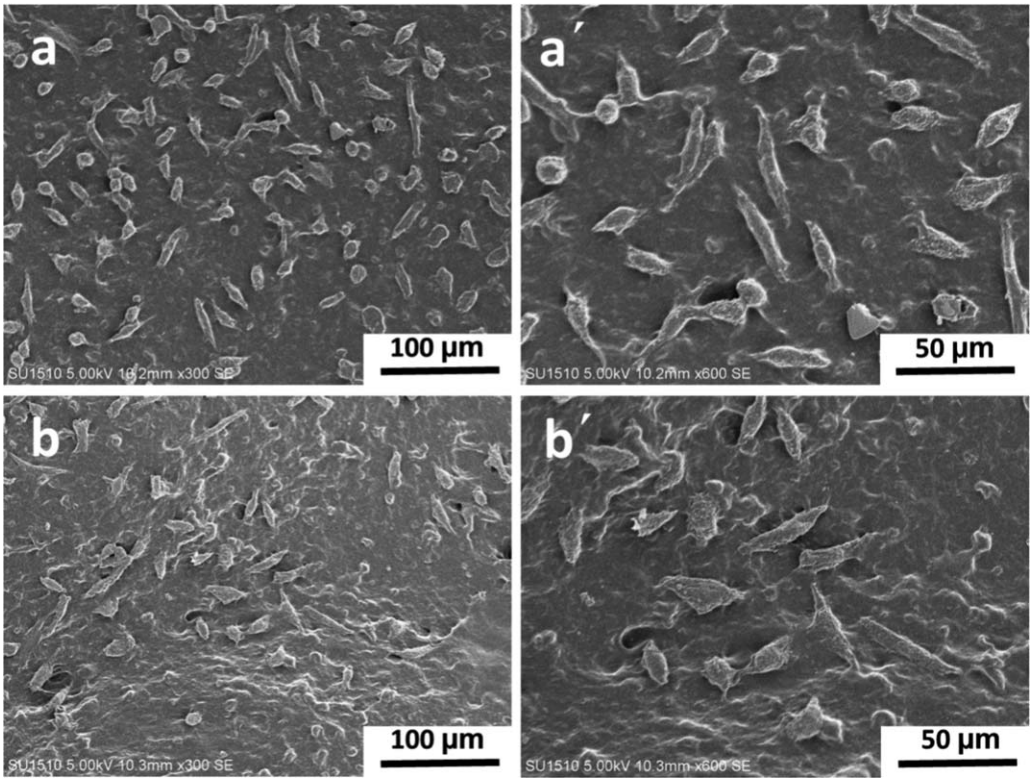

Figure 9. Cell attachment on (a) (a′) PVA-SbQ/zein nanofibers and (b) (b′) PVA-SbQ/zein/drug nanofibers.

structures were softened, which was caused by the weakening of hydrogen bonds between the amino and carbonyl groups in the backbone of zein and vaccarin.

Degradation and Surface Wettability Measurement

Figure 6 shows the in vitro degradation profiles of electrospun nanofibers from PVA-SbQ/zein blend with different blending ratios in a phosphate buffer solution (pH 7.4) at 37°C. It is apparent that the electrospun membranes were degraded with the time increased. Depending on the blending ratio, the electrospun membranes showed various degradation rates. For example, the in vitro degradation in 14 days reached ~28% for the membrane of PVA-SbQ/zein (1 : 1). However, the degradation of PVA-SbQ/zein (4 : 1) nanofibers was lower with a degradation of 26% after 21 days. This was probably because the lower zein content contributed little to the degradation of nanofibers and the coalescence between nanofibers adversed to the degradation. The results of water hydrolytic analysis revealed that the electrospun PVA-SbQ/zein composite membranes had good *in vitro* degradability.[39]

The hydrophilic/hydrophobic characteristics of the nanofibers can influence the initial adhesion of cells and their proliferation to a higher extent.[3] For this reason, water contact angles of zein, PVA-SbQ/zein, PVA-SbQ/zein/drug nanofibers were conducted, as shown in Figure 7. With an increase of PVA-SbQ amount and a decrease of zein amount, the water contact angle was found to decrease. It was because zein has a more hydrophobic character due to more hydrophobic non-polar amino acids than polar hydrophilic ones.[40] A more hydrophilic nanofiber surface will be helpful for cells attachment and could provide a moist environment to accelerate the wound healing. However, a more hydrophilic nanofiber surface may result in poor fiber stability and low tensile strength. Therefore, an optimized amount of zein should be considered to keep good surface wettability and fiber stability. The ratio of PVA-SbQ/zein (1 : 1) was chosen for cell viability and cell attachment tests, which is consistent with the surface morphology results in Figure 1.

Cell Viability and Cell Attachment

A primary requirement for wound healing materials is that it must be biocompatible, which is the ability of the material to perform with an appropriate host response in a specific situation.[41] The biocompatibility of the PVA-SbQ/zein nanofibers with and without drug was examined by measuring cytotoxicity after indirect and direct contact, and the results are shown in Figure 8. As shown in Figure 8(a) and 8b, the nanofibers with drug and without drug showed non-toxic impact on L929 cells and the cells were growing normally and exhibited normal morphology.[42,43] After 24 h incubation with extracts of the PVA-SbQ/zein and PVA-SbQ/zein/drug nanofibers, cell viability was 110.7% and 120.7% in the condition of low concentration, respectively. After 72 h incubation, cell viability was 93.3% and 137.4%. This was due to the vaccarin could promote the cell proliferation. In addition, the low concentration of DMEM provided the best condition for cell growth than the other two concentrations.

The attachment of L929 cells on the nanofibers was analyzed using SEM. Figure 9(a,b) showed the attached cells on the surface of PVA-SbQ/zein and PVA-SbQ/zein/drug nanofibers. The images revealed that the L929 cells maintained a fusiform morphology on the composite nanofibers with and without drug. These results demonstrated that the nanofibers are biocompatible and safe for using as wound healing materials.[44]

CONCLUSIONS

Electrospun PVA-SbQ/zein nanofibrous membranes with and without vaccarin drug were successfully fabricated. The obtained composite membranes were characterized with various methods. Comprehensive consideration of surface morphology, tensile strength, degradation, and surface wettability of different ratios of PVA-SbQ/zein nanofibers, the ratio of PVA-SbQ/zein (1 : 1) was selected as the optimized one. TG results showed that the stability of drug cladding in the nanofibers could be improved. After the incorporation of vaccarin, the components showed compatibility in the nanofibers, which could be verified from the FTIR analysis. Cell viability and cell attachment showed that both the PVA-SbQ/zein and PVA-SbQ/zein/drug nanofibers had good biocompatibility and cell adhesion. The nanofibers added vaccarin drug could also promote the cell proliferation, which would be used for wound healing materials.

ACKNOWLEDGMENTS

This research was financially supported by the National Natural Science Foundation of China (51006046, 51203064, 21201083, and 51163014), Jiangsu Province (2012-XCL-007), and International Joint Research Laboratory for Advance Functional Textile Materials of Jiangnan University, Changjiang Scholars and Innovative Research Team in University (IRT1135), the Priority Academic Program Development of Jiangsu Higher Education Institutions and the Innovation Program for Graduate Education in Jiangsu Province (CXZZ13_07).

REFERENCES

1. Kontogiannopoulos, K. N.; Assimopoulou, A. N.; Tsivintzelis, I.; Panayiotou, C.; Papageorgiou, V. P. *Int. J. Pharm.* **2011**, *409*, 216.
2. Wharram, S. E.; Zhang, X. H.; Kaplan, D. L.; McCarthy, S. P. *Macromol. Biosci.* **2010**, *10*, 246.
3. Lin, J.; Li, C.; Zhao, Y.; Hu, J.; Zhang, L. M. *ACS Appl. Mater. Interface* **2012**, *4*, 1050.
4. Abrigo, M.; McArthur, S. L.; Kingshott, P. *Macromol. Biosci.* **2014**, *14*, 772.
5. Karuppuswamy, P.; Venugopal, J. R.; Navaneethan, B.; Laiva, A. L.; Sridhar, S.; Ramakrishna, S. *Appl. Surf. Sci.* **2014**, *322*, 162.
6. Bhattarai, N.; Edmondson, D.; Veiseh, O.; Matsen, F. A.; Zhang, M. Q. *Biomaterials* **2005**, *26*, 6176.
7. Shalumon, K. T.; Anulekha, K. H.; Nair, S. V.; Nair, S. V.; Chennazhi, K. P.; Jayakumar, R. *Int. J. Biol. Macromol.* **2011**, *49*, 247.
8. Zou, B.; Liu, Y. W.; Luo, X. M.; Chen, F.; Guo, X. Q.; Li, X. H. *Acta Biomater.* **2012**, *8*, 1576.
9. Zhang, C. L.; Yu, S. H. *Chem. Soc. Rev.* **2014**, 4423.
10. Sahoo, S.; Ang, L. T.; Goh, J. C. H.; Toh, S. L. *J. Biomed. Mater. Res. Part A* **2010**, *93A*, 2010.
11. Croisier, F.; Atanasova, G.; Poumay, Y.; Jerome, C. *Adv. Healthcare Mater.* **2014**, *3*, 2032.
12. Jiang, Y. N.; Mo, H. Y.; Yu, D. G. *Int. J. Pharm.* **2012**, *438*, 232.
13. Hu, X.; Liu, S.; Zhou, G.; Huang, Y.; Xie, Z.; Jing, X. *J. Control. Release* **2014**, *185*, 12.
14. Lee, Y. J.; Lee, J. H.; Cho, H. J.; Kim, H. K.; Yoon, T. R.; Shin, H. *Biomaterials* **2013**, *34*, 5059.
15. Tang, C.; Saquing, C. D.; Morton, S. W.; Glatz, B. N.; Kelly, R. M.; Khan, S. A. *ACS Appl. Mater. Interfaces* **2014**, *6*, 11899.
16. Aytimur, A.; Kocyigit, S.; Uslu, I.; Gokmese, F. *Int. J. Polym. Mater. Polym. Biomat.* **2015**, *64*, 111.
17. Dai, L.; Long, Z.; Ren, X. H.; Deng, H. B.; He, H.; Liu, W. *J. Appl. Polym.* **2014**, *131*, 41051.
18. Unnithan, A. R.; Gnanasekaran, G.; Sathishkumar, Y.; Lee, Y. S.; Kim, C. S. *Carbohydr. Polym.* **2014**, *102*, 884.
19. Kayaci, F.; Uyar, T. *Carbohydr. Polym.* **2012**, *90*, 558.
20. Shukla, R.; Cheryan, M. *Ind. Crops Products* **2001**, *13*, 171.
21. Hurtado-Lopez, P.; Murdan, S. *J. Microencapsul.* **2006**, *23*, 303.
22. Neo, Y. P.; Ray, S.; Jin, J.; Gizdavic-Nikolaidis, M.; Nieuwoudt, M. K.; Liu, D.; Quek, S. Y. *Food Chem.* **2013**, *136*, 1013.
23. Paliwal, R.; Palakurthi, S. *J. Control. Release* **2014**, *189*, 108.
24. Selling, G. W.; Sessa, D. J.; Palmquist, D. E. *Polymer* **2004**, *45*, 4249.
25. Selling, G. W.; Woods, K. K.; Sessa, D.; Biswas, A. *Macromol. Chem. Phys.* **2008**, *209*, 1003.
26. Sessa, D. J.; Woods, K. K.; Mohamed, A. A.; Palmquist, D. E. *Ind. Crops Prod.* **2011**, *33*, 57.
27. Yao, C.; Li, X. S.; Song, T. Y. *J. Appl. Polym. Sci.* **2007**, *103*, 380.
28. Reddy, N.; Li, Y.; Yang, Y. Q. *Biotechnol. Prog.* **2009**, *25*, 139.
29. Kim, S.; Sessa, D. J.; Lawton, J. W. *Ind. Crops Prod.* **2004**, *20*, 291.
30. Wang, Q. Q.; Nandgaonkar, A. G.; Cui, J.; Huang, F. L.; Krause, W. E.; Lucia, L. A.; Wei, Q. F. *RSC Adv.* **2014**, *4*, 61573.
31. Ichimura, K.; Iwata, S.; Mochizuki, S. Y.; Ohmi, M.; Adachi, D. *J. Polym. Sci. Part A: Polym. Chem.* **2012**, *50*, 4094.
32. Tao, Y.; Ai, L.; Bai, H.; Liu, X. *J. Polym. Sci. Part A: Polym. Chem.* **2012**, *50*, 3507.
33. Xu, J.; Bai, H. Y.; Wang, M.; Xia, W. S.; Liu, X. Y. *Polym. Polym. Compos.* **2013**, *21*, 55.
34. Liu, Y.; Bolger, B.; Cahill, P. A.; McGuinness, G. B. *Mater. Lett.* **2009**, *63*, 419.
35. Xie, F.; Cai, W.; Liu, Y.; Li, Y.; Du, B.; Feng, L.; Qiu, L. *Int. J. Mol. Med.* **2015**, *35*, 135.
36. Naseri, N.; Algan, C.; Jacobs, V.; John, M.; Oksman, K.; Mathew, A. P. *Carbohydr. Polym.* **2014**, *109*, 7.

37. Wang, Y. L.; Guo, G.; Chen, H. F.; Gao, X.; Fan, R. R.; Zhang, D. M.; Zhou, L. X. *Int. J. Nanomed.* **2014**, *9*, 1991.

38. Yu, D. G.; Wang, X.; Li, X. Y.; Chian, W.; Li, Y.; Liao, Y. Z. *Acta Biomater.* **2013**, *9*, 5665.

39. Fu, S. Z.; Ni, P. Y.; Wang, B. Y.; Chu, B. Y.; Peng, J. R.; Zheng, L.; Zhao, X.; Luo, F.; Wei, Y. Q.; Qian, Z. Y. *Biomaterials* **2012**, *33*, 8363.

40. Sousa, F. F. O.; Luzardo-Alvarez, A.; Blanco-Mendez, J.; Otero-Espinar, F. J.; Martin-Pastor, M.; Macho, I. S. *Eur. J. Pharm. Biopharm.* **2013**, *85*, 790.

41. Mohamad, N.; Amin, M.; Pandey, M.; Ahmad, N.; Rajab, N. F. *Carbohydr. Polym.* **2014**, *114*, 312.

42. Guo, G.; Fu, S. Z.; Zhou, L. X.; Liang, H.; Fan, M.; Luo, F.; Qian, Z. Y.; Wei, Y. Q. *Nanoscale* **2011**, *3*, 3825.

43. Ji, X. Y.; Yang, W. J.; Wang, T.; Mao, C.; Guo, L. L.; Xiao, J. Q.; He, N. Y. *J. Biomed. Nanotechnol.* **2013**, *9*, 1672.

44. Yang, W. J.; Fu, J.; Wang, D. X.; Wang, T.; Wang, H.; Jin, S. G.; He, N. Y. *J. Biomed. Nanotechnol.* **2010**, *6*, 254.